Angewandte Chemie
Eine Zeitschrift der Gesellschaft Deutscher Chemiker

Supporting Information

69451 Weinheim, Germany

Exceptional Negative Thermal Expansion of Metal-Organic Frameworks

David Dubbeldam[1], Krista S. Walton[2], Donald E. Ellis[3], and Randall Q. Snurr[1]

[1] Chemical and Biological Engineering Department, Northwestern University, 2145 Sheridan Road, Evanston IL 60208 USA
[2] Department of Chemical Engineering, Kansas State University 1017 Durland Hall Manhattan, KS 66506 USA
[3] Department of Physics and Astronomy, Northwestern University, 2145 Sheridan Road, Evanston IL 60208 USA

1 Flexible Metal-Organic Frameworks

Metal-organic frameworks, sometimes referred to as coordination polymers, are a new class of nanoporous materials synthesized in a building-block approach from metal or metal-oxide vertices interconnected by organic linkers [1, 2, 3, 4, 5]. The organic linker molecules are typically rigid and contain two or three functional groups symmetrically arranged at the ends of the molecules. Many MOFs exhibit permanent microporosity and many are stable up to several hundred degrees Celsius, thus mimicking some of the prime features of zeolites. The isoreticular metal-organic frameworks (IRMOFs) have oxide-centered Zn_4O tetrahedra at the corners edge-bridged by six carboxylates to produce three dimensional, cubic, porous structures as shown in Figure S1.

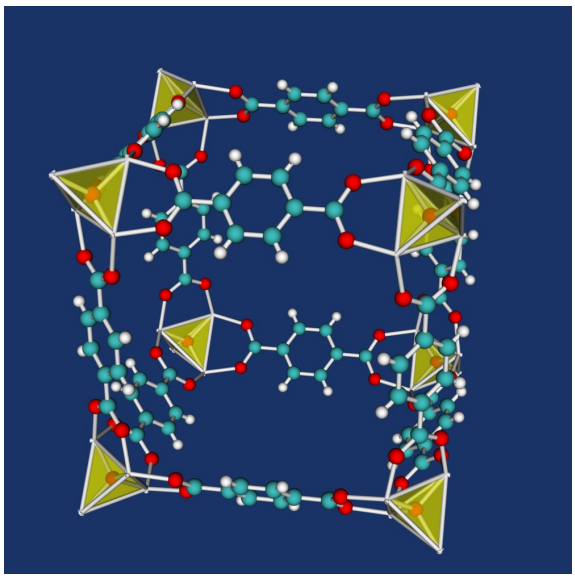

Figure S1: IRMOF-1 with the Zn_4O tetrahedra (shown in yellow) linked by 1, 4-benzenedicarboxylates. IRMOF-1 contains two alternating cavities of about 10.9 Å and 14.3 Å in diameter. The latter is shown here where the linkers are pointing "outwards". Other IRMOFs differ in the nature of functional groups decorating the pores and in the length of the linker molecule.

2 A New Model for Flexible MOFs

IRMOFs all have the same cubic structure and differ in the linker molecules. In Figure S2 we show the linkers for IRMOF-1, IRMOF-10 and IRMOF-16. The crystallographically different atoms are labeled; the other labels follow by symmetry.

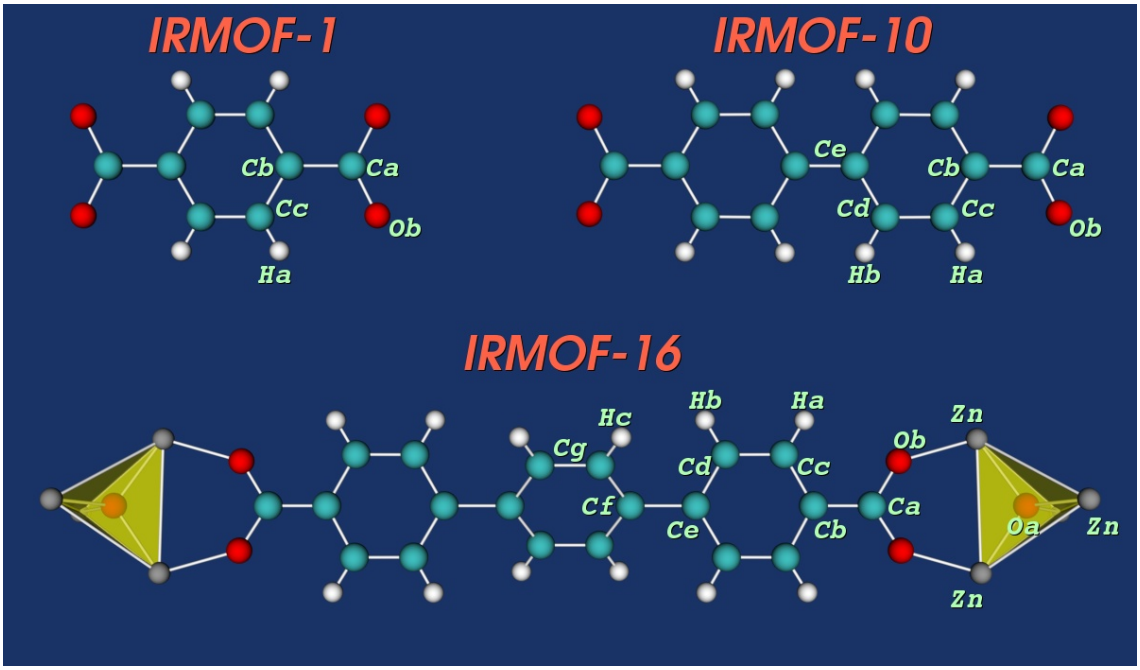

Figure S2: The definitions of the crystallographically different atoms in the linker molecules for IRMOF-1,10 and 16. The linker of IRMOF-16 is shown connected to the Zn_4O tetrahedra. The oxygens are shown in red, zinc in silver, carbon in cyan, and hydrogen in white.

Force field

The model is based on a combination of two pre-existing models:

1. A model for the Zn_4O metal-oxide cluster
   Metal-oxides are very successfully modeled using the Core-Shell method [6, 7, 8]. To model polarization on the oxygen, the charge of the oxygen is divided over the "core" and the "shell" which are separated by a spring. Typically, a Buckingham potential is used for the metal (with no attraction term), while for the oxygen both the exponential repulsion and the r^{-6} attraction term are used. The attraction of the oxygen is very strong (see Ref. [9] for a compilation of metal-oxide parameters).

2. A model for the linker molecule
   For the linker molecule a variety of models are readily available: AMBER [10, 11, 12, 13, 14], OPLS [15, 16, 17, 18], AMBER/OPLS [19, 20, 21, 22], CHARMM [23, 24, 25], GROMOS [26, 27, 28], CVFF [29], CFF [30, 31, 32], MM2 [33, 34, 35], MM3 [36, 37], MM4 [38, 39, 40, 41, 42, 43], MMFF94 [44, 45, 46, 47, 48, 49], DREIDING [50], COMPASS [51], PCFF [51], UFF [52], etc.

The combination of the two models is not straightforward:

1. The metal-oxide Zn_4O in a MOF is *not* part of an extended oxide structure anymore.

2. The bond lengths of the linker molecule in the MOF may be different from the gas and/or liquid-phase values.

3. For a generic model, we would like to have a single type of van der Waals potential using mixing rules for unlike interactions. It is difficult to combine Buckingham with Lennard-Jones potentials.

We therefore decided on the following strategy:

1. The Zn_4O cluster is refitted using Lennard-Jones and Coulombic potentials. The Lennard-Jones ϵ parameter for the oxygen is taken to be very large, while the ϵ for the Zn-metal is taken to be very small (resembling almost no attraction). The σ Lennard-Jones size parameters are varied until satisfactory agreement with the crystal structure is obtained for atom-atom distances and angles.

2. The linker molecule equilibrium bond distances and angles are modified where needed to obtain agreement with the crystal structure, while the bond, bend, torsions, and improper torsion force-constants were taken from the CVFF forcefield.

3. There are experimental crystal-structure data for IRMOF-1 at 169K for an evacuated structure (almost no solvent DMF molecules present). Experimentally, the crystal unit cell size is easier to determine then the bond distances and angles, and have preference in the fitting procedure. We initially set our goals to predict the crystal structure size within 0.01 Å, bond distances within 0.01 Å, and angles within 2°. However, we also wanted to have a single model describing IRMOF-1, 10, and 16 and decided to relax this condition on the bond lengths.

4. We would like to predict adsorption –accurately– using the *same* model. This required an iterative fitting procedure, i.e. for every structure that predicted the crystal structure the predicted adsorption of CO_2 and methane was checked. Alteration of the parameters to match adsorption leads to a different crystal structure and the parameters are further modified to reproduce the crystal structure again etc.

Note that in contrast to the work of Greathouse and Allendorf [53] we treat the oxygen Ob in the linker molecules as belonging to the linker molecule. In the work of Greathouse and Allendorf the oxygen Oa and Ob have identical parameters and can therefore be considered part of the metal-oxide cluster. Quantum mechanical simulations indicated the charge of the Ob is very different from Oa, and in fact equivalent to what is found for a gas-phase linker molecule. Therfore, in our opinion the split into a linker molecule and the Zn_4O is the most natural one. The functional form of the force field is shown in Table S1, and the bonded parameters in Table S2, S3, and S4 for IRMOF-1, IRMOF-10, and IRMOF-16, respectively. The nonbonded parameters are listed in Table S5, and the parameters for methane and CO_2 are given in Table S6.

$U^{\text{total}} = U^{\text{bonded}} + U^{\text{nonbonded}}$	
$U^{\text{bonded}} = U^{\text{bond}} + U^{\text{bend}} + U^{\text{torsion}} + U^{\text{imp. torsion}}$	
bond energy	$U^{\text{bond}}\left(r_{ij}\right) = \sum_{\text{bonds}} \frac{1}{2} k \left(r_{ij} - r_0\right)^2$
bend energy	$U^{\text{bend}}\left(\theta_{ijk}\right) = \sum_{\text{bends}} \frac{1}{2} k \left(\theta_{ijk} - \theta_0\right)^2$
torsion energy	$U^{\text{torsion}}\left(\phi_{ijkl}\right) = \sum_{\text{torsions}} k \left[1 + \cos\left(m\phi_{ijkl} - \phi_0\right)\right]$
improper torsion energy	$U^{\text{imp. torsion}}\left(\phi_{ijkl}\right) = \sum_{\text{imp. tors.}} k \left[1 + \cos\left(m\phi_{ijkl} - \phi_0\right)\right]$
$U^{\text{nonbonded}} = U^{\text{VDW}} + U^{\text{Ewald}}$	
Van der Waals energy	$U^{\text{VDW}} = \sum_{i<j} \begin{cases} 4\epsilon_{ij}\left[\left(\frac{\sigma_{ij}}{r_{ij}}\right)^{12} - \left(\frac{\sigma_{ij}}{r_{ij}}\right)^{6}\right] - E_{\text{cut}} & \text{if } r < r_{\text{cut}} \\ 0 & \text{if } r \geq r_{\text{cut}} \end{cases}$
Ewald charge energy	$U^{\text{Ewald}} = U^{\text{real}} + U^{\text{rec}} + U^{\text{self}} + U^{\text{exclusion}}$ where $U^{\text{real}} = \sum_{i<j} q_i q_j \frac{\text{erfc}\left(\alpha r_{ij}\right)}{r_{ij}}$ $U^{\text{rec}} = \frac{2\pi}{V} \sum_{\mathbf{k}\neq 0} \frac{1}{k^2} e^{-\frac{k^2}{4\alpha^2}} \left(\left\lvert\sum_{i=1}^{N} q_i \cos\left(\mathbf{k}\cdot\mathbf{r}_i\right)\right\rvert^2 + \left\lvert\sum_{i=1}^{N} q_i \sin\left(\mathbf{k}\cdot\mathbf{r}_i\right)\right\rvert^2\right)$ $U^{\text{self}} = -\sum_i \frac{\alpha}{\sqrt{\pi}} q_i^2$ $U^{\text{exclusion}} = -\sum_{i<j} q_i q_j \frac{\text{erf}\left(\alpha r_{ij}\right)}{r_{ij}}$

Table S1: Functional forms of the force field for flexible IRMOFs. Note that 1-2 and 1-3 interactions between neighbors are skipped in the VDW and Ewald real-part, and a correction to the Fourier sum is made. The Lennard-Jones potentials are cut at $r_{\text{cut}} = 12$ Å, and shifted with E_{cut} the energy at the cutoff. For adsorption using Monte Carlo the adsorbate-adsorbate interactions used truncated interactions plus tail corrections when the literature sorbate-sorbate model was developed this way, e.g. CO_2.

Force field: bonded interactions

bond					bend						torsion								improper torsion							
i	j	k/k_B	r_0 [Å]	#	i	j	k	k/k_B	θ_0 [°]	#	i	j	k	l	k/k_B [K]	ϕ_0 [°]	m [-]	#	i	j	k	l	k/k_B [K]	ϕ_0 [°]	m [-]	#
Ob	Ca	543840.0	1.27	96	Ob	Ca	Ob	135960.0	132	48	Ob	Ca	Cb	Cc	1258.9	180	2	96	Cb	Ca	Ob	Ob	5036.0	180	2	48
Ca	Cb	353750.0	1.44	48	Ob	Ca	Cb	54882.0	114	96	Ca	Cb	Cc	Ha	1510.7	180	2	96	Cc	Cb	Cc	Ca	5037.0	180	2	48
Cb	Cc	483414.0	1.365	96	Ca	Cb	Cc	34927.0	120	96	Ca	Cb	Cc	Cc	1510.7	180	2	96	Cb	Cc	Cc	H	186.3	180	2	96
Cc	Cc	483414.0	1.365	48	Cc	Cb	Cc	90640.0	120	48	Cb	Cc	Cc	Ha	1510.7	180	2	96								
Cc	Ha	366000.0	0.95	96	Cc	Cc	Cb	90640.0	120	96	Cb	Cc	Cc	Cb	1510.7	180	2	48								
					Cb	Cc	Ha	37263.0	120	96	Cc	Cb	Cc	Cc	1510.7	180	2	96								
					Cc	Cc	Ha	37263.0	120	96	Ha	Cc	Cb	Cc	1510.7	180	2	96								
											Ha	Cc	Cc	Ha	1510.7	180	2	48								
											Ha	Cb	Cc	Ha	1510.7	180	2	96								

Table S2: IRMOF-1 bonded parameters: 424 atoms, 384 bonds, 576 angles, 768 torsions, 192 improper torsions, and 960 excluded interactions per unit cell. Note that the parameters are a subset of IRMOF-16. Bond constants in units of K/Å^2, bend constants in units of K/degree^2.

bond					bend						torsion								improper torsion							
i	j	k/k_B	r_0 [Å]	#	i	j	k	k/k_B	θ_0 [°]	#	i	j	k	l	k/k_B [K]	ϕ_0 [°]	m [-]	#	i	j	k	l	k/k_B [K]	ϕ_0 [°]	m [-]	#
Ob	Ca	543840.0	1.27	96	Ob	Ca	Ob	135960.0	132	48	Ob	Ca	Cb	Cc	1258.9	180	2	96	Ca	Cb	Cc	Cc	5035.6	180	2	48
Ca	Cb	353750.0	1.44	48	Ob	Ca	Cb	54882.0	114	96	Ca	Cb	Cc	Cd	1510.7	180	2	96	Cb	Ca	Ob	Ob	5035.6	180	2	48
Cb	Cc	483414.0	1.365	96	Ca	Cb	Cc	34927.0	120	96	Ca	Cb	Cc	Ha	1510.7	180	2	96	Cb	Cc	Cd	Ha	186.3	180	2	96
Cc	Cd	483414.0	1.365	96	Cb	Cc	Cd	90640.0	120	96	Cb	Cc	Cd	Hb	1510.7	180	2	96	Cc	Cd	Ce	Hb	186.3	180	2	96
Cd	Ce	483414.0	1.365	96	Cc	Cb	Cc	90640.0	120	48	Cb	Cc	Cd	Ce	1510.7	180	2	96	Cd	Ce	Cd	Ce	186.3	180	2	48
Ce	Ce	483414.0	1.365	24	Cc	Cd	Ce	90640.0	120	96	Cc	Cb	Cc	Cd	1510.7	180	2	96								
Cc	Ha	366000.0	0.95	96	Cd	Ce	Cd	90640.0	120	48	Cc	Cd	Ce	Cd	1510.7	180	2	96								
Cd	Hb	366000.0	0.95	96	Cd	Ce	Ce	90640.0	120	96	Cc	Cd	Ce	Ce	1510.7	180	2	96								
					Cd	Cc	Ha	37263.0	120	96	Cc	Cb	Cc	Cd	1510.7	180	2	96								
					Cb	Cc	Ha	37263.0	120	96	Cc	Cd	Ce	Cd	1510.7	180	2	96								
					Cc	Cd	Hb	37263.0	120	96	Cd	Ce	Cd	Hb	1510.7	180	2	96								
					Ce	Cd	Hb	37263.0	120	96	Cd	Ce	Ce	Cd	1510.7	180	2	96								
											Ce	Cd	Cc	Ha	1510.7	180	2	96								
											Ce	Ce	Cd	Hb	1510.7	180	2	96								
											Hb	Cd	Cc	Ha	1510.7	180	2	96								

Table S3: IRMOF-10 bonded parameters: 664 atoms, 648 bonds, 1008 angles, 1440 torsions, 336 improper torsions, and 1656 excluded interactions per unit cell. Note that the parameters are a subset of IRMOF-16. Bond constants in units of K/Å^2, bend constants in units of K/degree^2.

bond					bend						torsion								improper torsion							
i	j	k/k_B	r_0 [Å]	#	i	j	k	k/k_B	θ_0 [°]	#	i	j	k	l	k/k_B [K]	ϕ_0 [°]	m [-]	#	i	j	k	l	k/k_B [K]	ϕ_0 [°]	m [-]	#
Ob	Ca	543840.0	1.27	96	Ob	Ca	Ob	135960.0	132	48	Ob	Ca	Cb	Cc	1258.9	180	2	96	Cb	Ca	Ob	Ob	5035.6	180	2	48
Ca	Cb	353750.0	1.44	48	Ob	Ca	Cb	54882.0	114	96	Ca	Cb	Cc	Cd	1510.7	180	2	96	Cc	Cd	Ce	Hb	186.3	180	2	96
Cb	Cc	483414.0	1.365	96	Ca	Cb	Cc	34927.0	120	96	Ca	Cb	Cc	Cc	1510.7	180	2	96	Cb	Cc	Cd	Ha	186.3	180	2	96
Cc	Cd	483414.0	1.365	96	Cb	Cc	Cd	90640.0	120	96	Cb	Cc	Cd	Hb	1510.7	180	2	96	Cb	Cc	Cd	Ha	186.3	180	2	96
Cd	Ce	483414.0	1.365	96	Cc	Cb	Cc	90640.0	120	48	Cb	Cc	Cd	Ce	1510.7	180	2	96	Cd	Ce	Cd	Cf	186.3	180	2	48
Ce	Cf	483414.0	1.46	48	Cc	Cd	Ce	90640.0	120	96	Cc	Cb	Cc	Ha	1510.7	180	2	96	Ce	Cf	Cg	Cg	186.3	180	2	48
Cf	Cg	483414.0	1.365	96	Cd	Ce	Cd	90640.0	120	48	Cc	Cb	Cc	Cd	1510.7	180	2	96	Cf	Cg	Cg	Hc	186.3	180	2	96
Cg	Cg	483414.0	1.365	48	Cd	Ce	Cf	90640.0	120	96	Cc	Cd	Ce	Cd	1510.7	180	2	96								
Cc	Ha	366000.0	0.95	96	Ce	Cf	Cg	90640.0	120	96	Cc	Cd	Ce	Cf	1510.7	180	2	96								
Cd	Hb	366000.0	0.95	96	Cf	Cg	Cg	90640.0	120	96	Cd	Ce	Cd	Hb	1510.7	180	2	96								
Cg	Hc	366000.0	0.95	96	Cg	Cf	Cg	90640.0	120	48	Cd	Ce	Ce	Cd	1510.7	180	2	96								
					Cb	Cc	Ha	37263.0	120	96	Cd	Ce	Cf	Cg	1510.7	180	2	96								
					Cd	Cc	Ha	37263.0	120	96	Ce	Cd	Cc	Ha	1510.7	180	2	96								
					Cc	Cd	Hb	37263.0	120	96	Ce	Cf	Cg	Hc	1510.7	180	2	96								
					Ce	Cd	Hb	37263.0	120	96	Ce	Cf	Cg	Cg	1510.7	180	2	96								
					Cf	Cg	Hc	37263.0	120	96	Cf	Ce	Cd	Hb	1510.7	180	2	96								
					Cg	Cg	Hc	37263.0	120	96	Cf	Cg	Cg	Hc	1510.7	180	2	96								
											Cf	Cg	Cg	Cf	1510.7	180	2	96								
											Cg	Cf	Cg	Hc	1510.7	180	2	96								
											Cg	Cf	Cg	Cg	1510.7	180	2	96								
											Ha	Cc	Cd	Hb	1510.7	180	2	96								
											Hc	Cg	Cg	Hc	1510.7	180	2	96								

Table S4: IRMOF-16 bonded parameters: 904 atoms, 912 bonds, 1440 angles, 2112 torsions, 480 improper torsions, and 2352 excluded interactions per unit cell. Bond constants in units of K/Å^2, bend constants in units of K/degree^2.

Force field: non-bonded interactions

MOF-atoms			
atom type	ϵ/k_B [K]	σ [Å]	charge IRMOF-1,10,16 [a.u.]
Zn	0.42	2.7	1.275
Oa	700	2.98	-1.5
Ob	70.5	3.11	-0.6
Ca	47.0	3.74	0.475
Cb	47.86	3.47	0.125
Cc	47.86	3.47	-0.15
Cd	47.86	3.47	-0.15
Ce	47.86	3.47	0.0
Cf	47.86	3.47	0.0
Cg	47.86	3.47	-0.15
Ha	7.65	2.85	0.15
Hb	7.65	2.85	0.15
Hc	7.65	2.85	0.15

Table S5: Nonbonded Van der Waals and charge parameters for the adsorbents used in this work. The ϵ Lennard-Jones parameter is given in units of Kelvin. To convert to kJ/mol, multiply by $R/1000$ with $R \approx 8.314464919$ J mol^{-1} K^{-1} the gas-constant.

carbondioxide (CO_2)			
atom type	ϵ/k_B [K]	σ [Å]	charges
C	28.129	2.757	0.6512
O	80.507	3.033	-0.3256
methane (CH_4)			
atom type	ϵ/k_B [K]	σ [Å]	charges
CH_4	148	173	-

Table S6: Nonbonded Van der Waals and charge parameters for the adsorbates used in this work. The EPM2-model for CO_2 is used because of its remarkable accuracy of the phase equilibrium [54]. Also the TraPPE model for methane is optimized to reproduce the vapor-liquid phase equilibrium [55].

Charges were calculated in Gaussian [56] using the pbepbe functional. This uses the Perdew, Burke, and Ernzerhof functional for both exchange and correlation [57]. A 6-31+g* basis set was used, this includes one polarization (*) and one diffuse (+) function on all atoms except hydrogen. The charges were obtained with the Chelpg method [58]. This method relies on atomic radii which must be provided. In this work these were taken from Bondi et al. [59]. We used clusters based on the experimental crystal structures and had one organic linker and two metal clusters that were terminated by methyl groups. These methyl groups were given a standard sp3 geometry.

Parameterization discussion

There are various force fields for rigid MOFs which do reproduce adsorption isotherms (from reasonably well up to excellent). The model of Yang and Zhong for example reproduces the adsorption of methane and CO_2 in IRMOF-1 [60]. However, this is achieved by using a different parameter set depending whether methane or CO_2 is used. Another example is the DREIDING model. Test simulations using this model shows that when extending the model to include flexibility, the metal-clusters fly apart due to the large size of the zinc. The model clearly needs to be reparameterized if used for a flexible framework. Although rigid models can reproduce adsorption, they are ambiguous because different parameter sets can give the same adsorption. The solution of Yang and Zhong to use different parameters depending upon the adsorbate lacks transferability.

The ambiguity largely disappears when the model is reparameterized for a flexible model. The Lennard-Jones σ-values of the framework generally determine the inter-atomic distances, while adsorption is mostly dependent on the ϵ values. The tradeoffs of σ and ϵ, as can be made in rigid models (since the σ-dependence is largely ignored by the rigid-approximation), vanish for flexible models. Inflections in adsorption isotherms provide a very sensitive parameterization method [61, 62]. Skoulidas and Sholl [63] adopt the point of view that "the accuracy of a force field for adsorption in a nanoporous material should also imply a reasonable

level of confidence in the same force field for predicting diffusive properties." We tend to agree. For example our value for the diffusion of benzene in IRMOF-1 at 298K and 80 mg/g (about 6 molecules per unit cell) is approximately $4.28 \pm 0.57 \times 10^{-9}$ m^2/s for our flexible model, in very good agreement with the experimental value of 1.8×10^{-9} or 2×10^{-9} m^2/s depending on the measurement parameters [64].

3 Simulation Details

3.1 Structure prediction

The simulations for the structure prediction have been run using NPT (constant number of atoms N, constant average pressure P, constant average temperature T) molecular dynamics simulations for at least 10 nanoseconds using a time step of 0.5 femtoseconds. The pressure (1 atm) and temperature correspond to the experimental conditions. The NPT algorithm uses the reversible measure-preserving integrator NPT method of Martyna et al. [65]. Charges are computed using the Ewald summation. Test results of 2x2x2 unit cell systems were found to be equivalent to 1x1x1 results, but deemed to be too expensive for production runs. The runs were performed using 1x1x1 unit cells with high relative Ewald precision of 10^{-8} for IRMOF-1 ($\alpha = 0.317887$ and $\mathbf{k}_{\max} = \{10, 10, 10\}$), and medium precision of 10^{-6} for IRMOF-10 and IRMOF-16 ($\alpha = 0.265058$, $\mathbf{k}_{\max} = \{9, 9, 9\}$ and $\alpha = 0.265058$, $\mathbf{k}_{\max} = \{12, 12, 12\}$ respectively). Simulations using the NPT Monte Carlo algorithm gave equivalent results.

3.2 Adsorption simulations

In adsorption studies one would like to know the amount of molecules adsorbed as a function of pressure and temperature of the reservoir with which the adsorbent is in contact. Therefore the natural ensemble to use is the grand-canonical ensemble (or μ, V, T ensemble). In this ensemble, the temperature T, the volume V, and the chemical potential μ are fixed. The equilibrium conditions are that the temperature and chemical potential of the gas inside and outside the adsorbent must be equal. The imposed chemical potential μ can be related to the fugacity f computed directly from the equation of state of the vapor in the reservoir. For most adsorbates, the experimental equation of state is well known and we use the Peng-Robinson equation of state to convert the pressure to the corresponding fugacity.

To obtain an isotherm using a flexible framework we need to perform Monte Carlo moves that change the internal conformation of the framework as well as changing the volume. The ensemble can therefore be considered to be μPT.

- Framework atom translation
  We randomly select a framework atom and give it a random displacement [66]. The maximum displacement is taken such that 50% of the moves are accepted. The acceptance rule is

$$\text{acc}\,(\text{old} \rightarrow \text{new}) = \min\left(1, e^{-\beta\left(U^{\text{new}} - U^{\text{old}}\right)}\right). \tag{1}$$

  Note that this scheme works for zeolites but is insufficient for MOFs because concerted movement, such as the rotation of the phenyl-group in a linker molecule, is not accounted for using individual atom moves.

- Hybrid move
  We perform a small NVE molecular dynamics run of M time steps to obtain a new configuration [67]. The acceptance rule is

$$\text{acc}\,(\text{old} \rightarrow \text{new}) = \min\left(1, e^{-\beta\left(U^{\text{new}} - U^{\text{old}}\right)}\right). \tag{2}$$

  Note that $\Delta U = U^{\text{new}} - U^{\text{old}}$ is the integration error. In relative units this error is quite small, but not in absolute units, i.e. with $M = 5$ and $\Delta t = 0.5$ fs for the CO_2 isotherm this results in an acceptance of approximately 80%. Our adsorption isotherms are computed with at least 0.5 ns of total MD-time during the simulation.

- Volume move
  If we perform a random walk in $\ln V$, the probability of finding volume V is given by

$$\mathcal{N}\left(\ln(V);\mathbf{s}^N\right) \propto e^{-\beta(PV+U)+(N+1)\ln V} \tag{3}$$

  For a random walk in $\ln V$, instead of in V, the domain of this walk coincides with all possible values of V [68]. Furthermore, the average step size turns out to be less sensitive to the density. The acceptance criterion is based on the difference of enthalpies:

$$\Delta H = \Delta U + P\left(V^{\text{new}} - V^{\text{old}}\right) - (N+1)\frac{1}{\beta}\ln\frac{V^{\text{new}}}{V^{\text{old}}} \tag{4}$$

$$\text{acc}\,(\text{old} \rightarrow \text{new}) = \min\left(1, e^{-\beta\Delta H}\right) \tag{5}$$

  To change the volume we scale all the framework atoms "atomically', all flexible adsorbates "atomically" and all rigid adsorbates "molecularly". Molecular scaling changes the center of mass of the molecule but leaves the internal configuration untouched.

- Other moves
  The usual GCMC moves of adsorbate translation, rotation, and biased regrow, insertion and deletion were performed [68], see Table S7.

move	total trials	total grown	total accepted	acceptance [%]	displacement
translation in x-direction	1001062	-	499329	49.8799	0.770169
translation in y-direction	1000668	-	499772	49.9438	0.751786
translation in z-direction	1000322	-	502396	50.2234	0.823668
random rotation	3339152	-	559905	16.767880	-
regrow	3340265	3005633	140718	4.212780	-
insertion	3036011	2719998	376168	12.390205	-
deletion	3036605	3036605	376166	12.387716	-
volume	109001	-	47834	43.884001	0.008616
hybrid	110000	-	88982	80.892727	-

Table S7: GCMC statistics for CO_2 at 40 bar and 298K (saturation loading).

The runs were performed using one unit cell consisting of 8 cages with medium relative Ewald precision of 10^{-6} ($\alpha = 0.265058$ and $\mathbf{k}_{\text{max}} = \{7,7,7\}$ wave vectors for IRMOF-1). The Monte Carlo results were verified by performing μPT molecular dynamics simulations. Here, during an NPT molecular dynamics particles are swapped in and out every $M = 5$ time steps to apply a chemical potential corresponding to the applied pressure. Both methods were found to be in excellent agreement.

4 Validation

4.1 Crystal structure

Selected bond lengths

atom	atom	exp. 258K [69]	sim. 258K	exp. 169K [70]	sim. 169K
Oa	Zn	1.941	1.964	1.9498	1.962
Ob	Zn	1.922	1.942	1.9378	1.935
Zn	Zn	3.171	3.204	3.185	3.203
Ob	Ca	1.301	1.275	1.262	1.275
Ca	Cb	1.486	1.502	1.50	1.501
Cb	Cc	1.392	1.404	1.383	1.403
Cc	Cc	1.388	1.391	1.369	1.391
Cc	Ha	0.927	0.958	0.973	0.957

Table S8: Selected bond lengths in units of Å for IRMOF-1

atom	atom	exp. 258K [69]	sim. 258K
Oa	Zn	1.947	1.961
Ob	Zn	1.952	1.943
Zn	Zn	3.177	3.201
Ob	Ca	1.279	1.275
Ca	Cb	1.441	1.502
Cb	Cc	1.391	1.403
Cc	Cd	1.403	1.391
Cd	Ce	1.403	1.404
Ce	Ce	1.413	1.420
Cc	Ha	0.959	0.958
Cd	Hb	0.96	0.954

Table S9: Selected bond lengths in units of Å for IRMOF-10

atom	atom	exp. 258K [69]	sim. 258K
Oa	Zn	1.935	1.959
Ob	Zn	1.936	1.945
Zn	Zn	3.16	3.199
Ob	Ca	1.239	1.275
Ca	Cb	1.38	1.501
Cb	Cc	1.386	1.404
Cc	Cd	1.392	1.391
Cd	Ce	1.398	1.400
Ce	Cf	1.549	1.505
Cf	Cg	1.405	1.400
Cc	Ha	0.95	0.957
Cd	Hb	0.95	0.953
Cg	Hc	0.95	0.953

Table S10: Selected bond lengths in units of Å for IRMOF-16

Selected bond angles

atom	atom	atom	exp. 258K [69]	sim. 258K	exp. 169K [70]	sim. 169K
Zn	Ob	Ca	129.5	129.4	131.0	129.7
Oa	Zn	Ob	112.55	110.2	111.28	110.5
Ob	Zn	Ob	106.2	108.4	107.6	108.2
Zn	Oa	Zn	109.5	109.4	109.4712	109.4
Ob	Ca	Cb	116.8	116.8	117.04	116.8
Ob	Ca	Ob	126.4	126.1	125.9	126.1
Ca	Cb	Cc	120.0	121.4	120.74	121.4
Cb	Cc	Cc	120.0	121.3	120.74	121.4
Cc	Cb	Cc	119.9	117.0	118.5	117.0
Cc	Cc	Ha	119.9	117.8	120.08	117.8
Cb	Cc	Ha	120.1	120.4	119.18	120.5

Table S11: Selected bond angles in degrees for IRMOF-1

4.2 Thermal properties

The volumetric expansion coefficient is defined as

$$\beta = \frac{1}{V}\left(\frac{\partial V}{\partial T}\right)_P \tag{6}$$

and the linear thermal expansion coefficient of a bar of length L as

$$\alpha = \frac{1}{L}\left(\frac{\partial L}{\partial T}\right)_P \tag{7}$$

For isotropic materials

$$\beta = 3\alpha \tag{8}$$

In an NPT simulation we can compute the volumetric expansion coefficient from a fluctuation formula as [71]

$$\beta = \frac{1}{V}\left(\frac{\partial V}{\partial T}\right)_{NP} = \frac{1}{k_B T^2 \langle V\rangle_{NPT}}\left[\langle VH\rangle_{NPT} - \langle V\rangle_{NPT}\langle H\rangle_{NPT}\right] \tag{9}$$

The simulations for IRMOF-1 using the fluctuation formula were run for at least 15 ns for each temperature.

References

[1] Eddaoudi, M.; Moler, D.B.; Li, H.; Chen, B.; Reineke, T.M.; O'Keeffe, M.; Yaghi, O.M. *Acc. Chem. Res.* **2001**, *34*, 319-330.

[2] James, S.L. *Chem. Soc. Rev.* **2003**, *32*, 276-288.

[3] Janiak, C. *Dalton Trans.* **2003**, *14*, 2781-2804.

[4] Yaghi, O. M.; O'Keeffe, M.; Ockwig, N. W.; Chae, H. K.; Eddaoudi, M.; Kim, J. *Nature* **2003**, *423*, 705-714.

[5] Rowsell, J. L. C.; Yaghi, O.M. *Micropor. Mesopor. Mater.* **2004**, *73*, 3-14.

[6] Dick, B.G.; Overhauser, A.W. *Phys. Rev.* **1958**, *112*, 90-103.

[7] Catlow, C. R. A.; Cormack, A. N.; Theobald, F. *Acta Cryst. B* **1984**, *40*, 195-200.

[8] Schroder, K. P.; Sauer, J. *J. Phys. Chem.* **1996**, *100*, 11043-11049.

[9] Woodley, S. M.; Battle, P. D.; Gale, J. D.; Catlow, C. R. A. *Phys. Chem. Chem. Phys.* **1999**, *1*, 2535-2542.

[10] Cornell, W. D.; Cieplak, P.; Bayly, C. I.; Gould, I. R.; Merz Jr., K. M.; Ferguson, D. M.; Spellmeyer, D. C.; Fox, T.; Caldwell, J. W.; Kollman, P. A. *J. Am. Chem. Soc.* **1992**, *117*, 5179-5197.

[11] Pearlman, D. A.; Case, D. A.; Caldwell, J. C.; Seibel, G. L.; Singh, U. C.; Weiner, P.; Kollman, P. A., *AMBER 4.0* University of California Press; San Francisco, 1991.

[12] Weiner, P. K.; Kollman, P. A. *J. Comp. Chem.* **1981**, *2*, 287-303.

[13] Weiner, S. J.; Kollman, P. A.; Case, D. A.; Singh, U. C.; Ghio, C.; Alagona, G.; Profeta Jr., S.; Weiner, P.K. *J. Am. Chem. Soc.* **1984**, *106*, 765-784.

[14] Weiner, S. J.; Kollman, P. A.; Nguyen, D. T.; Case, D. A. *J. Comp. Chem.* **1986**, *7*, 230-252.

[15] Jorgensen, W. L.; Madura, J. D.; Swenson, C. J. *J. Am. Chem. Soc.* **1984**, *106*, 6638.

[16] Jorgensen, W. L.; Swenson, C. J. *J. Am. Chem. Soc.* **1985**, *107*, 569.

[17] Jorgensen, W. L. *J. Phys. Chem.* **1986**, *90*, 6379.

[18] Jorgensen, W. L. *J. Phys. Chem.* **1986**, *90*, 1276.

[19] Damm, W.; Frontera, A.; Tirado-Rives, J.; Jorgensen, W. L. *J. Comp. Chem.* **1997**, *18*, 1955-1970.

[20] Jorgensen, W. L.; Maxwell, D. S.; Tirado-Rives, J. *J. Am. Chem. Soc.* **1996**, *118*, 11225-11236.

[21] Jorgensen, W. L.; Tirado-Rives, J. *J. Am. Chem. Soc.* **1988**, *110*, 1657-1666.

[22] Kaminski, G.; Duffy, E. M.; Matsui, T.; Jorgensen, W. L. *J. Phys. Chem.* **1994**, *98*, 13077-13082.

[23] MacKerell, A. D.; Bashford, D.; Bellott, M.; Dunbrack, R. L.; Evanseck, J. D.; Field, M. J.; Fischer, S.; Gao, J.; Guo, H.; Ha, S.; Joseph-McCarthy, D.; Kuchnir, L.; Kuczera, K.; Lau, F. T. K.; Michnick, C. Mattos S.; Ngo, T.; Nguyen, D. T.; Prodhom, B.; Reiher, W. E.; Roux, B.; Schlenkrich, M.; Smith, J. C.; Stote, R.; Straub, J.; Watanabe, M.; Wiorkiewicz-Kuczera, J.; Yin, D.; Karplus, M. *J. Phys. Chem. B* **1998**, *102*, 3586-3617.

[24] Momany, F. A.; Rone, R. *J. Comp. Chem.* **1992**, *13*, 888-900.

[25] Pavelites, J. J.; Gao, J.; Bash, P.A.; Mackerell Jr., A. D. *J. Comp. Chem.* **1997**, *18*, 221-239.

[26] Hermans, J.; Berendsen, H. J. C.; van Gunsteren, W. F.; Postma, J. P. M. *Biopolymers* **1984**, *23*, 1-.

[27] Ott, K.-H.; Meyer, B. *J. Comp. Chem.* **1996**, *17*, 1068-1084.

[28] van Gunsteren, W. F.; Daura, X.; Mark, A. E. *Encyclopaedia of Computational Chemistry* **1997**, *17*, .

[29] Dauber-Osguthorpe, P.; Roberts, V. A.; Osguthorpe, D. J.; Wolff, J.; Genest, M.; Hagler, A. T. *Proteins: Structure, Function and Genetics* **1988**, *4*, 31-47.

[30] Hagler, A. T.; Ewig, C. S. *Comp. Phys. Comm.* **1994**, *84*, 131-155.

[31] Hwang, M.-J.; Stockfisch, T. P.; Hagler, A. T. *J. Am. Chem. Soc.* **1994**, *116*, 195 -231.

[32] Maple, J. R.; Hwang, M.-J; Stockfisch, T. P.; Hagler, A. T. *Israel J. Chem.* **1994**, *34*, 195 -231.

[33] Allinger, N. L. *J. Am. Chem. Soc.* **1977**, *99*, 8127-8134.

[34] Allinger, N. L.; Kok, R.; Imam, M. R. *J. Comp. Chem.* **1988**, *9*, 591-595.

[35] Lii, J.-H.; Gallion, S.; Bender, C.; Wikstrom, H.; Allinger, N. L.; Flurchick, K. M.; Teeter, M. M. *J. Comp. Chem.* **1989**, *10*, 503-513.

[36] Lii, J.-H.; Allinger, N. L. *J. Comp. Chem.* **1991**, *12*, 186-199.

[37] Lii, J.-H.; Allinger, N. L. *J. Comp. Chem.* **1998**, *19*, 1001-1016.

[38] Allinger, N. L.; Chen, K.; Lii, J.-H. *J. Comp. Chem.* **1996**, *17*, 642-668.

[39] Allinger, N. L.; Chen, K.; Katzenellenbogen, J. A.; Wilson, S. R.; Anstead, G. M. *J. Comp. Chem.* **1996**, *17*, 747-755.

[40] Allinger, N. L.; Fan, Y. *J. Comp. Chem.* **1997**, *18*, 1827-1847.

[41] Nevens, N.; Chen, K.; Allinger, N. L. *J. Comp. Chem.* **1996**, *17*, 669-694.

[42] Nevens, N.; Lii, J.-H.; Allinger, N. L. *J. Comp. Chem.* **1996**, *17*, 695-729.

[43] Nevens, N.; Allinger, N. L. *J. Comp. Chem.* **1996**, *17*, 730-746.

[44] Halgren, T. A. *J. Am. Chem. Soc.* **1992**, *114*, 7827-7843.

[45] Halgren, T. A. *J. Comp. Chem.* **1996**, *17*, 490-519.

[46] Halgren, T. A. *J. Comp. Chem.* **1996**, *17*, 520-552.

[47] Halgren, T. A. *J. Comp. Chem.* **1996**, *17*, 553-586.

[48] Halgren, T. A.; Nachbar, R. B. *J. Comp. Chem.* **1996**, *17*, 587-615.

[49] Halgren, T. A.; Nachbar, R. B. *J. Comp. Chem.* **1996**, *17*, 616-641.

[50] Mayo, S. L.; Olafson, B. D.; Goddard, W. A. *J. Phys. Chem.* **1990**, *94*, 8897-8909.

[51] Sun, H.; Ren, P.; Fried, J. R. *Computational and Theoretical Polymer Sciences* **1998**, *8*, 229-246.

[52] Rappé, A. K.; Casewit, C. J.; Colwell, K. S.; Goddard, W. A.; Skiff, W. M. J. *J. Am. Chem. Soc.* **1992**, *114*, 10024-10035.

[53] Greathouse, J. A.; Allendorf, M. D. *J. Am. Chem. Soc.* **2006**, *128*, 10678-10679.

[54] Harris, J. G.; Yung, K. H. *J. Phys. Chem.* **1995**, *99*, 12021-12024.

[55] Martin, M. G.; Siepmann, J. I. *J. Phys. Chem. B* **1998**, *102*, 2569-2577.

[56] Frisch, M. J.; Trucks, G. W.; Schlegel, H. B.; Scuseria, G. E.; Robb, M. A.; Cheeseman, J. R.; Montgomery, J. A. Jr.; Vreven, T.; Kudin, K. N.; Burant, J. C.; Millam, J. M.; Iyengar, S. S.; Tomasi, J.; Barone, V.; Mennucci, B.; Cossi, M.; Scalmani, G.; Rega, N.; Petersson, G. A.; Nakatsuji, H.; Hada, M.; Ehara, M.; Toyota, K.; Fukuda, R.; Hasegawa, J.; Ishida, M.; Nakajima, T.; Honda, Y.; Kitao, O.; Nakai, H.; Klene, M.; Li, X.; Knox, J. E.; Hratchian, H. P.; Cross, J. B.; Bakken, V.; Adamo, C.; Jaramillo, J.; Gomperts, R.; Stratmann, R. E.; Yazyev, O.; Austin, A. J.; Cammi, R.; Pomelli, C.; Ochterski, J. W.; Ayala, P. Y.; Morokuma, K.; Voth, G. A.; Salvador, P.; Dannenberg, J. J.; Zakrzewski, V. G.; Dapprich, S.; Daniels, A. D.; Strain, M. C.; Farkas, O.; Malick, D. K.; Rabuck, A. D.; Raghavachari, K.; Foresman, J. B.; Ortiz, J. V.; Cui, Q.; Baboul, A. G.; Clifford, S.; Cioslowski, J.; Stefanov, B. B.; Liu, G.; Liashenko, A.; Piskorz, P.; Komaromi, I.; Martin, R. L.; Fox, D. J.; Keith, T.; Al-Laham, M. A.; Peng, C. Y.; Nanayakkara, A.; Challacombe, M.; Gill, P. M. W.; Johnson, B.; Chen, W.; Wong, M. W.; Gonzalez, C.; Pople, J. A., Gaussian 03, Revision C.02, Gaussian, Inc., Wallingford, CT, 2004.

[57] Perdew, J. P.; Burke, K.; Ernzerhof, M. *Phys. Rev. Lett.* **1996**, *77*, 3865-3868.

[58] Reed, A. E.; Curtiss, L. A.; Weinhold, F. *Chem. Rev.* **1988**, *88*, 899-926.

[59] Bondi, A. *J. Phys. Chem.* **1964**, *68*, 441.

[60] Yang, Q. Y.; Zhong, C. L. *J. Phys. Chem. B* **2006**, *110*, 17776-17783.

[61] Dubbeldam, D.; Calero, S.; Vlugt, T. J. H.; Krishna, R.; Maesen, T. L. M.; Beerdsen, E.; Smit, B. *Phys. Rev. Lett.* **2004**, *93*, 088302-1.

[62] Dubbeldam, D.; Calero, S.; Vlugt, T. J. H.; Krishna, R.; Maesen, T. L. M.; Smit, B. *J. Phys. Chem. B* **2004**, *108*, 12301-12313.

[63] Skoulidas, A. I.; Sholl, D. S. *J. Phys. Chem. B* **2005**, *109*, 15760-15768.

[64] Stallmach, F.; Gröger, S.; Künzel, V.; Kärger, J.; Yaghi, O. M.; Hesse, M.; Müller, U. *Angew. Chem. Int. Ed.* **2006**, *45*, 2123-2126.

[65] Martyna, G. J.; Tuckerman, M.; Tobias, D. J.; Klein, M. L. *Mol. Phys.* **1996**, *87*, 1117-1157.

[66] Vlugt, T. J. H.; Schenk, M. *J. Phys. Chem. B* **2002**, *106*, 12757-12763.

[67] Chempath, S.; Clark, L. A.; Snurr, R. Q. *J. Chem. Phys.* **2003**, *118*, 7635-7643.

[68] Frenkel, D.; Smit, B., *Understanding Molecular Simulation 2nd edition* Academic Press; London, UK, 2002.

[69] Eddaoudi, M.; Kim, J.; Rosi, N.; Vodak, D.; Wachter, J.; O'Keefe, M.; Yaghi, O. M. *Science* **2002**, *295*, 469-472.

[70] Li, H.; Eddaoudi, M.; O'Keeffe, M.; Yaghi, O. M. *Nature* **1999**, *402*, 276-279.

[71] Allen, M. P.; Tildesley, D. J., *Computer Simulation of Liquids* Clarendon Press; Oxford, 1987.